

RESEARCH ARTICLE

Mutation in Mg-Protoporphyrin IX Monomethyl Ester Cyclase Decreases Photosynthesis Capacity in Rice

Xuexia Wang^{1,2}, Rongfeng Huang^{1,2}, Ruidang Quan^{1,2*}

1 Biotechnology Research Institute, Chinese Academy of Agricultural Sciences, Beijing, China, **2** National Key Facility of Crop Gene Resources and Genetic Improvement, Beijing, China

* quanruidang@caas.cn



OPEN ACCESS

Citation: Wang X, Huang R, Quan R (2017) Mutation in Mg-Protoporphyrin IX Monomethyl Ester Cyclase Decreases Photosynthesis Capacity in Rice. PLoS ONE 12(1): e0171118. doi:10.1371/journal.pone.0171118

Editor: Steven M. Theg, University of California - Davis, UNITED STATES

Received: August 14, 2016

Accepted: January 15, 2017

Published: January 27, 2017

Copyright: © 2017 Wang et al. This is an open access article distributed under the terms of the [Creative Commons Attribution License](https://creativecommons.org/licenses/by/4.0/), which permits unrestricted use, distribution, and reproduction in any medium, provided the original author and source are credited.

Data Availability Statement: All relevant data are within the paper and its Supporting Information files.

Funding: Support was provided by the Ministry of Agriculture of China (2014ZX08009-005, 2016ZX08009-003-005 to RQ) [<http://english.agri.gov.cn/>] and the National Natural Science Foundation of China (31172025 to RQ) [<http://www.nsf.gov.cn/>]. The funders had no role in study design, data collection and analysis, decision to publish, or preparation of the manuscript.

Abstract

In photosynthesis, the pigments chlorophyll a/b absorb light energy to convert to chemical energy in chloroplasts. Though most enzymes of chlorophyll biosynthesis from glutamyl-tRNA to chlorophyll a/b have been identified, the exact composition and regulation of the multimeric enzyme Mg-protoporphyrin IX monomethyl ester cyclase (MPEC) is largely unknown. In this study, we isolated a rice pale-green leaf mutant *m167* with yellow-green leaf phenotype across the whole lifespan. Chlorophyll content decreases 43–51% and the granal stacks of chloroplasts becomes thinner in *m167*. Chlorophyll fluorescence parameters, including Fv/Fm (the maximum quantum efficiency of PSII) and quantum yield of PSII (Y(II)), were lower in *m167* than those in wild type plants (WT), and photosynthesis rate decreases 40% in leaves of *m167* mutant compared with WT plants, which lead to yield reduction in *m167*. Genetic analysis revealed that yellow-green leaf phenotype of *m167* is controlled by a single recessive genetic locus. By positional cloning, a single mutated locus, G286A (Alanine 96 to Threonine in protein), was found in the coding sequence of LOC_Os01g17170 (*Rice Copper Response Defect 1*, *OsCRD1*), encoding a putative sub-unit of MPEC. Expression profile analysis demonstrated that *OsCRD1* is mainly expressed in green tissues of rice. Sequence alignment analysis of CRD1 indicated that Alanine 96 is very conserved in all green plants and photosynthetic bacteria. *OsCRD1* protein mainly locates in chloroplast and the point mutation A96T in *OsCRD1* does not change its location. Therefore, Alanine96 of *OsCRD1* might be fundamental for MPEC activity, mutation of which leads to deficiency in chlorophyll biosynthesis and chloroplast development and decreases photosynthetic capacity in rice.

Introduction

Photosynthesis is the process of converting light energy to chemical energy and is the most important source of energy on the earth [1]. Chlorophyll (Chl) molecules harvest light energy for photosynthesis, so Chls are key cofactors for the photosynthetic apparatus [2].

The Chl biosynthesis pathway, including more than 17 enzymes in higher plants [3–7], comprises four distinct sections: common steps, heme/chlorophyll branch, chlorophyll cycle

Competing Interests: The authors have declared that no competing interests exist.

and chlorophyll breakdown [5]. The common steps start from 5-aminolevulinic acid (5-ALA) to protoporphyrin IX, which is a common precursor for Chl and heme biosynthesis [6, 7]. Chl branch starts from the insertion of Mg²⁺ into protoporphyrin IX by Mg chelatase to get Mg-protoporphyrin IX (MgP), followed by conversion to Mg-protoporphyrin IX monomethyl ester (MgPME) by a methyl transferase. Then, MgPME is used as a substrate for the Mg-protoporphyrin monomethyl ester cyclase (MPEC; EC 1.14.13.81) and creates protochlorophyllide (Pchl_{id}) [8].

In the process of Chl biosynthesis, MPEC is one of the least understood enzymes. The first study on MPEC was carried out in cucumber (*Cucumis sativus*) [9]. MPEC is a multiprotein complex consisting of at least two subunits in cucumber [9]. Further research found that one of the soluble component of MPEC is over 30 kD [10]. An oxidative cyclase component of MPEC AcsF was firstly cloned from *Rubrivivax gelatinosus* [11]. From various organisms, using biochemical and genetic approaches, people have identified many AcsF homologs, such as *Chlamydomonas reinhardtii copper response defect 1 (Crd1)* [12], *Pharbitis nil Leu zipper (PNZIP)* [13], *Epipremnum aureum ZIP* [14], *Nicotiana tabacum ZIP and Arabidopsis thaliana CHL27* [15], *Hordeum vulgare Xantha-l* [16]. In *Arabidopsis*, CHL27 involves in the conversion of MgPME to Pchl_{id}, and leaves of either the antisense or T-DNA mutant are chlorotic or yellow, and chloroplast development is defected accompanied with PSI and PSII instability. [15, 17].

Low Chlorophyll Accumulation A (LCAA), with the Ycf54 domain, interacts with and stabilizes CHL27 protein in tobacco, which indicates LCAA may be another component of MPEC [18]. In *Synechocystis* YCF54-like protein (Ycf54), a potential component of MPEC identified by separate pulldown assay using two FLAG-tagged ACSF homologs as baits, is essential for the activity and stability of the oxidative cyclase [19]. Similarly, barley Ycf54, associating with XanL, also stimulates MPEC activity [20]. In addition, barley Viridis-k might be an additional membrane associated component of the MPEC [16, 20]. So far, the components of barley MPEC consist of a soluble protein and three membrane-bound components, Ycf54, Xanth-l and unknown Viridis-k [16, 20]. Therefore, MPEC is the only enzyme with unidentified components in chlorophyll biosynthesis.

In higher plants, all of mutants in MPEC subunits are chlorotic and dwarf [15–18, 20], indicating MPEC is essential for green plants. However, in most cereal crops like rice, MPEC has not been characterized genetically yet. In this study, we characterized a yellow-green leaf rice (*Oryza sativa*) mutant *m167* from a rice variety Kitaake. Young and mature leaves are yellow-green, chlorophyll content and photosynthesis rate decrease, and the chloroplast development is arrested in *m167* mutant. Map-based cloning revealed that there is a site-mutation in the coding region of *OsCRD1* gene encoding a putative subunit of MPEC.

Materials and Methods

Plant materials

The *m167* mutant was isolated from a EMS mutagenized population from the Japonica rice variety Kitaake. To construct the F₂ mapping population, the yellow-green leaf rice mutant *m167* was crossed with rice varieties Zhifu802 and Dular, respectively. And the F₂ population was planted in Langfang to collect yellow-green leaf segregating individuals for genotyping.

Genetic analysis and map-based cloning

For genetic analysis in F₁ and F₂ populations, leaf color (yellow-green or green) of seedlings at 3-week was check with eye, and the F₂ segregation ratios were analyzed by χ^2 test.

DNA was extracted from leaves using the CTAB method. About 0.5 leaf tissues were ground in liquid nitrogen, added CTAB extraction buffer (2% CTAB, 0.1 M Tris-Cl pH8.0, 20 mM EDTA pH 8.0, 1.4 M NaCl, 1% PVP4000), and incubated at 65°C for 15 min. Then, each sample was added 1 volume of chloroform/isoamyl alcohol (96:4) and vortexed thoroughly. After centrifugation the aqueous layer were transferred to a new tube, and DNA was precipitated with 0.7 volume of isopropanol, washed with 0.5 mL 70% ethanol, and finally dissolved in 200 μ L of water. Genotyping was performed by PCR using a set of SSR molecular markers from Gramene website (<http://www.gramene.org/markers/>). Polymorphic SSR markers between the two parent lines were screened by the size of PCR products. Then the polymorphic SSR markers were used to identify the genotype of F₂ progenies. Some of the SSR marker sequences were listed in [S1 Table](#).

Sequence analysis

Within the fine mapped chromosome region, candidate genes were screened according to the Rice Genome Annotation Project (<http://rice.plantbiology.msu.edu/>) and gene specific primers were designed accordingly ([S1 Table](#)). These primers were used to amplify the candidate genes from the *m167* mutant and wild type Kitaake. The PCR amplified products were sequenced to determine difference between *m167* and wild type plants.

Homologous sequences of *OsCRD1* were identified using the Blastp search program of the National Center for Biotechnology Information (<http://www.ncbi.nlm.nih.gov>) [21].

RNA extraction and quantitative real-time PCR

Total RNA was extracted from various tissues of Kitaake and *m167* plants using Ultrapure RNA Kit (Cwbiotech, Beijing, China). Approximately 1 mg of total RNA from each sample was used for first-strand cDNA synthesis. For quantitative real-time RT-PCR, first strand cDNAs were used as templates in reactions using SYBR Green PCR Master Mix (Abm) according to the manufacturer's instructions. *OsActin* gene was amplified as an internal control. Amplification of target genes were carried out using a real-time quantitative system (Bio-rad IQ5).

Quantitative analysis of chlorophyll content, photosynthesis rate and chlorophyll fluorescence

For chlorophyll content determination, leaf tissues of 2-week-old and 2-month-old *m167* mutant and Kitaake (wild type) grown in the field were collected, and ground in ice-cold 80% acetone. Residual plant debris was removed by centrifugation at 8000 g for 10 min. Supernatants were analyzed with a visible spectrometer and chlorophyll contents were calculated as described previously [22].

To determine photosynthesis parameters, the plants of wild type and *m167* were planted in greenhouse for about 20 d before photosynthesis measurement. Photosynthesis (P) and transpiration (T) rates were measured using a portable photosynthesis system (LI-6400XT) in the morning (9 to 11 AM). All of the photosynthetic measurements were taken at a constant air flow rate of 500 μ mol s⁻¹. The concentration of CO₂ was 400 μ mol CO₂ mol⁻¹ using the system's CO₂ injector and the temperature was maintained at 30°C, and the photosynthetic photon flux density was 800 μ mol (photon) m⁻² s⁻¹. Three measurements were made for each plant, and 5 plants were used for both the wild type and the mutant.

To determine chlorophyll fluorescence parameters, chlorophyll fluorescence in vivo was measured at room temperature on intact plant leaves at 4-week stage using a fluorometer (IMAGING-PAM, Waltz, Germany)[23]. Before measurements plants were dark adapted for

at least 30 minutes at room temperature. Then a weak modulated measuring light was applied to register the minimal fluorescence yield (F_0). And then a saturating light pulse was applied to determine maximum fluorescence (F_m) and variable fluorescence (F_v). The photosystem II efficiency $Y(II)$, quantum yield of light-induced non-photochemical quenching $Y(NPQ)$, and quantum yield of non-regulated energy dissipation $Y(NO)$ were calculated as following: $Y(II) = (F_m' - F) / F_m'$, $NPQ = (F_m - F_m') / F_m'$, $Y(NPQ) = 1 - Y(II) - 1 / (NPQ + 1 + qL(F_m / F_0 - 1))$, $Y(NO) = 1 / (NPQ + 1 + qL(F_m / F_0 - 1))$. The chlorophyll fluorescence data was captured by a fluorometer IMAGING-PAM controlled by ImagingWin v2.41 software.

Transmission electron microscopy (TEM) analysis

Leaf samples for TEM analysis were harvested from the wild type and *m167* at 20 d-stage. Fixation and polymerization of leaf samples were carried out as described previously [24]. The fresh leaf tissues were cut into pieces and fixed in a solution of 2% glutaraldehyde and further incubated overnight. After staining with uranyl acetate, tissues were further dehydrated in an ethanol series, and finally embedded in Spurr's medium prior to ultrathin sectioning. Samples were stained again and examined with a transmission electron microscope (JEOL JEM-1230).

Subcellular localization of OsCRD1 protein

The subcellular localization of OsCRD1 was determined by transient expression of GFP fusion protein. The coding sequence of OsCRD1 was fused with GFP in-frame into a 35S-GFP vector. And then the GFP-OsCRD1 plasmid was introduced into rice green tissue protoplasts by PEG [25]. The transformed protoplast cells were examined by a confocal microscope.

Determination of Chl precursors

The contents of chlorophyll precursors protoporphyrin IX (Proto IX), Mg-protoporphyrin IX / Mg-protoporphyrin IX monomethyl ester (MgP/MgPME) and protochlorophyllide (Pchl) were determined according to the method described previously [26–30]. Briefly, the seedlings of WT and *m167* mutant were grown at 28°C in the dark for two weeks. Then, the intact leaves (approximately 4.0 g fresh weight) were incubated overnight at 22°C in darkness with 10 mM ALA in 50 mM phosphate buffer (pH 7.0). After incubation for 18 h, the leaves were extracted in 80% alkaline acetone under dim green light, then centrifuged for 10 min at 20 000 g, 4°C. The absorbance of the supernatants was determined with a spectrophotometer. The relative contents of chlorophyll precursors Proto IX, MgP/MgPME and Pchl in *m167* mutant were calculated with those in WT were defined as 1.

CRISPR/Cas9 mediated knock-out of OsCRD1 in wild type Kitaake plants

To confirm whether OsCRD1 is the candidate gene for *m167* mutant, we constructed the *OsCRD1* knock-out plants by CRISPR/Cas9 [31, 32]. Two gRNA targets were chosen, the first target was AGGAGGGAGAGCTCCATGG, and the second was GAA–GATGGTGATGTACCTC.

Results

Reduced chlorophyll accumulation, lower photosynthesis rate and delayed chloroplast development in *m167* mutant

The *m167* mutant was isolated from a pool of EMS mutagenized *japonica* rice Kitaake. The *m167* mutant exhibits a yellow-green leaf phenotype throughout the whole developmental

span (Fig 1A–1D). Plant height and yield of *m167* decreased by 26% and 49%, respectively, compared to that of wild type (Table 1).

Moreover, we examined chlorophyll content and photosynthesis rate of *m167* mutant. The content of Chl a and Chl b was significantly reduced in *m167* compared with the wild-type Kitaake. The Chl, Chl a and Chl b contents of *m167* were only about 57%, 18% and 40% of those of the wild type at seedling stage, respectively. And the Chl, Chl a and Chl b contents of *m167* were only about 49%, 82% and 63% of those of the wild type at heading stage, respectively. In addition, the Chl a/b ratio of *m167* increased at seedling stage but decreased at heading stage compared to that of wild type, indicating that the Chla/Chlb balance was destroyed in *m167* mutant (Fig 1E and 1F).

There was a decrease of photosynthesis, including net photosynthetic rate, stomatal conductance, intercellular carbon dioxide concentration and transpiration rate (Fig 1G–1J), suggesting that lower photosynthesis capacity in *m167* mutant. Lower photosynthesis capacity is consistent with lower grain yield. In addition, these results indicate that the regulation of stomatal aperture is affected by the mutation of CRD1 gene, implying that chlorophyll deficiency in chloroplasts of guard cells might malfunction the stomatal regulations.

To investigate the photosynthetic capacity of photosystem II (PSII) in the *m167* mutant, we determined the chlorophyll fluorescence data of rice seedlings at 4-week stage by a chlorophyll fluorometer (IMAGING-PAM, Heinz Walz GmbH). Fv/Fm (the maximum quantum efficiency of PSII) in *m167* was about half of that in WT (Fig 2A), indicating the maximum photosynthetic capacity of PSII was damaged in *m167* by lacking of chlorophyll. In addition, we captured chlorophyll fluorescence parameters during illumination with actinic light at $186 \mu\text{mol m}^{-2} \text{s}^{-1}$ in a time-dependent manner (Fig 2B–2D). Quantum yield of PSII (Y(II)) was significantly lower in *m167* than that in WT (Fig 2B), and Y(II) increased more gently over time in *m167* than that in WT. In addition, quantum yield of light-induced non-photochemical quenching Y(NPQ) was also lower in *m167* than that in WT (Fig 2C), but quantum yield of non-regulated energy dissipation Y(NO) was much higher in *m167* than that in WT (Fig 2D). Y(II) and Y(NPQ) are decreased and Y(NO) is increased in *m167*, indicating the absorbed light energy are dissipated by Y(NO) in *m167* mutant. Therefore, the photosynthetic capacity of PSII was greatly damaged in *m167* mutant.

To investigate if the chloroplast development was affected in *m167* mutant, we investigated the ultrastructure of plastids in *m167* mutant and WT plants at 3-week-old seedlings using transmission electron microscopy (Fig 3). Granal stacks in the *m167* mutant appeared less dense and lacked granal membranes compared to those of WT in developing leaves. Therefore, in *m167* mutant the chloroplast development is partially impaired.

Map-based cloning of *m167* mutation site

To map the mutation site in *m167* mutant, two F₁ and F₂ populations were constructed by crossing *m167* to Dular and Zhefu802, respectively. Then, we calculated the ratio of green:yellow-green plants in F₁ and F₂ generations (Table 2). The segregation ratio indicates that the mutation of a single recessive genetic locus might cause the yellow-green leaf phenotype in the *m167* mutant.

The genetic mapping of *m167* mutation was performed using the F₂ population from *m167*×Dular cross. In initial mapping of the *m167* target gene, we used approximately 200 SSR markers evenly distributing on 12 chromosomes. The mutation was initially mapped between the markers Chr 1–21 and Chr 1–23 on the short arm of chromosome 1 (Chr 1 represents chromosome 1 and the number 21 and 23 represent the serial number of markers). And then we enlarged the population for fine mapping using 430 segregated recessive individuals from

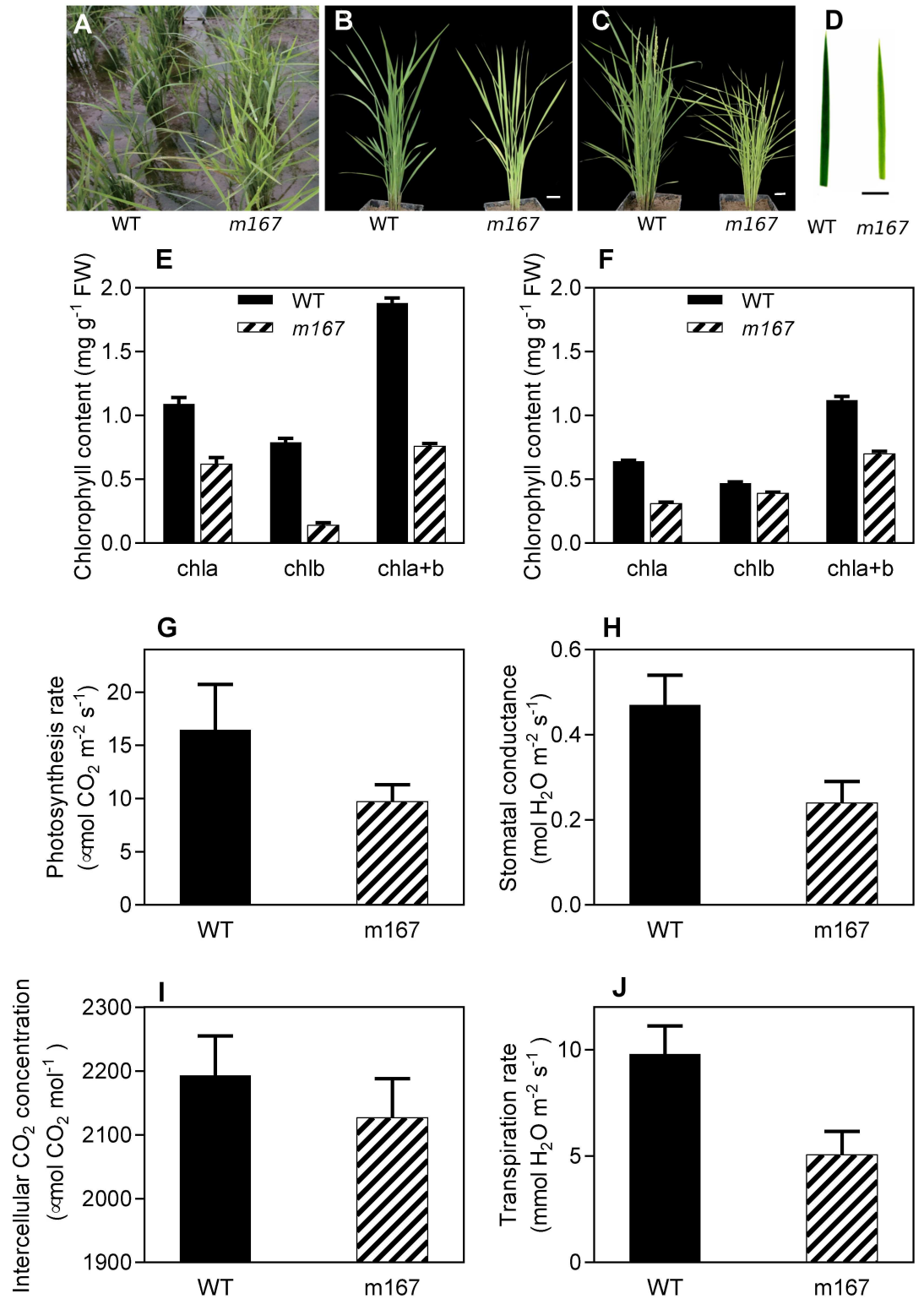


Fig 1. Physiological characterization of rice *m167* plants. A-D, *m167* shows yellow leaf at seedling (A and D), tillering (B), and heading stages (C). Bar = 5 cm. E-F, Leaf pigment contents of WT and *m167* at seedling (E) and heading stages (F). Chlorophyll contents data are mean ± SD (n = 3). G-J, Measurement of photosynthesis rate (G), stomatal conductance (H), intercellular CO₂ concentration (I) and transpiration rate (J) of wild type (WT) and *m167* rice plants.

doi:10.1371/journal.pone.0171118.g001

Table 1. The agronomic traits of *m167* and wild type Kitaake plants.

	Plant height (cm)	Spike length (cm)	Grain number per spike	Tilling number	Seed- setting rate (%)	1000- grain weight (g)	Yield per plant (g)
Kitaake	71.7±4.0	13.3±1.2	59.6±9.2	19.8±3.2	94.6±3.0	20.1±0.1	22.5±4.2
<i>m167</i>	52.4±1.8	11.7±0.9	42.4±8.	16.6±2.3	77.8±4.8	19.4±0.2	11.4±4.3

doi:10.1371/journal.pone.0171118.t001

F₂ population of *m167*×Dular. The mutation was located between markers MM2007 and MM2022 (<http://archive.gramene.org/markers/microsat/>). The mutation site was subsequently narrowed to a 73.36 kb region. Within this chromosomal region, nine open reading frames (ORFs) have been predicted according to the Rice Genome Annotation Project (<http://rice.plantbiology.msu.edu>) (S2 Table). All genes within this region were amplified and sequenced

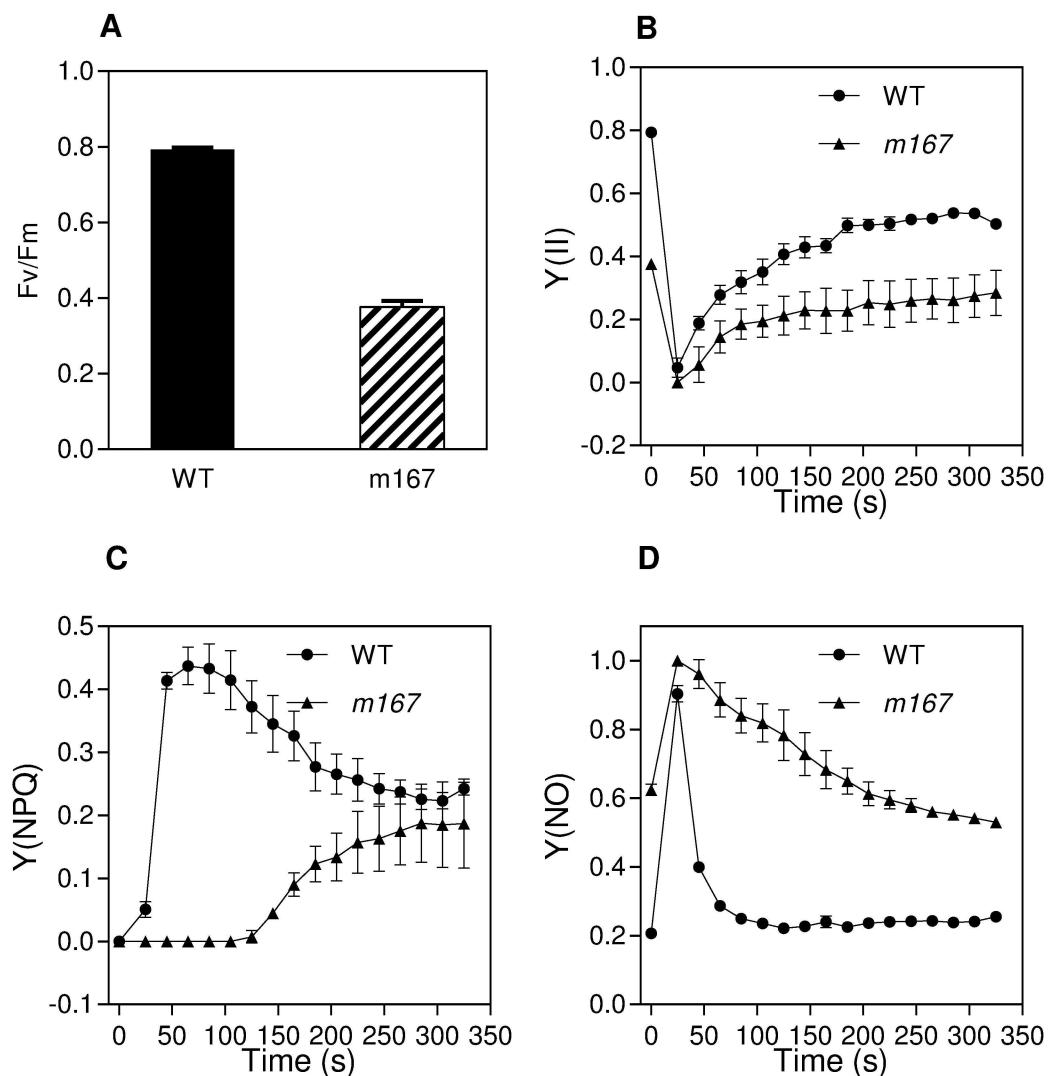


Fig 2. Chlorophyll fluorescence parameters of *m167* and WT plants. (A) Fv/Fm of leaves of *m167* and wild type plants. (B-D) Chlorophyll fluorescence kinetics including quantum yield of PSII Y(II) (B), quantum yield of light-induced non-photochemical quenching Y(NPQ) (C), and quantum yield of non-regulated energy dissipation Y(NO) (D) in leaves of *m167* and wild type plants. Data are means ± SD (n = 10).

doi:10.1371/journal.pone.0171118.g002

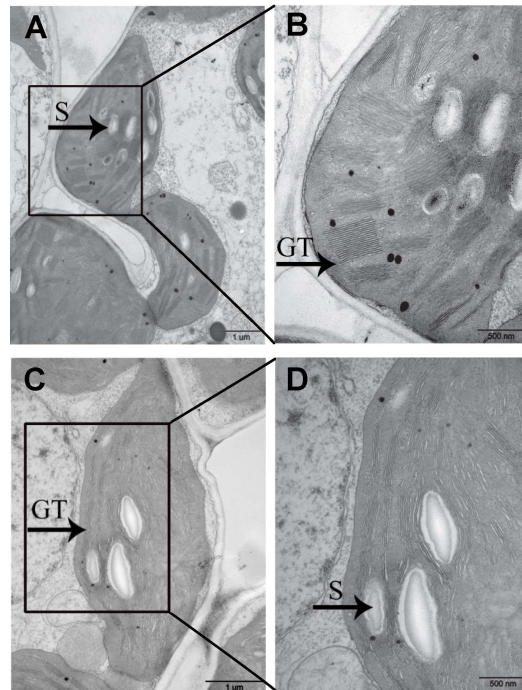


Fig 3. Transmission electron micrographs of chloroplasts. Transmission electron micrographs of chloroplasts in WT (A and B) and *m167* (C and D) plants. S and GT indicate starch granules and granal thylakoids, respectively.

doi:10.1371/journal.pone.0171118.g003

in *m167* and wild type Kitaake plants. A single nucleotide G-to-A substitution was found at position 286 in the coding region in the first exon of LOC_Os01g17170 (*OsCRD1*) in *m167* (Fig 4). This substitution changes amino acid 96 from alanine (A) to threonine (T) in *OsCRD1* protein. No sequence variations were detected in the genomic sequences of the other 8 candidates.

To verify the mutation of *OsCRD1* conferring yellow-green leaf in *m167*, we transferred *OsCRD1* genomic sequence to *m167* mutants, and found the pale green phenotype of *m167* was rescued. In addition, we also found that knocking out *OsCRD1* in wild type rice by CRISPR-Cas9 method caused leaf color to pale green (Fig 4E and 4F, S1 Fig).

All the above results demonstrate that the mutation in *OsCRD1* leads to leaf color change in *m167* mutant.

OsCRD1 belongs to a subunit of magnesium-protoporphyrin IX monomethyl ester cyclase

Blast search in the genome database revealed that *OsCRD1* is a single-copy gene in rice. In green plants, the number of CRD1 homologous genes alters in different species, with a single copy in most of crops but up to 17 copies in *Ostreococcus tauri* (GreenPhl v4, http://www.greenphyl.org/cgi-bin/family.cgi?p=id&family_id=2552#tab-famcomp). *OsCRD1* has an open

Table 2. Segregation of F₁ and F₂ populations from two crosses.

	F ₁		F ₂		
	Percentage of green plants	No. of yellow- green plants	No. of green plants	Ratio	χ ²
<i>m167</i> ×Dular	100%	194	634	1:3.27	0.316
<i>m167</i> ×Zhefu802	100%	105	370	1:3.52	2.196

doi:10.1371/journal.pone.0171118.t002

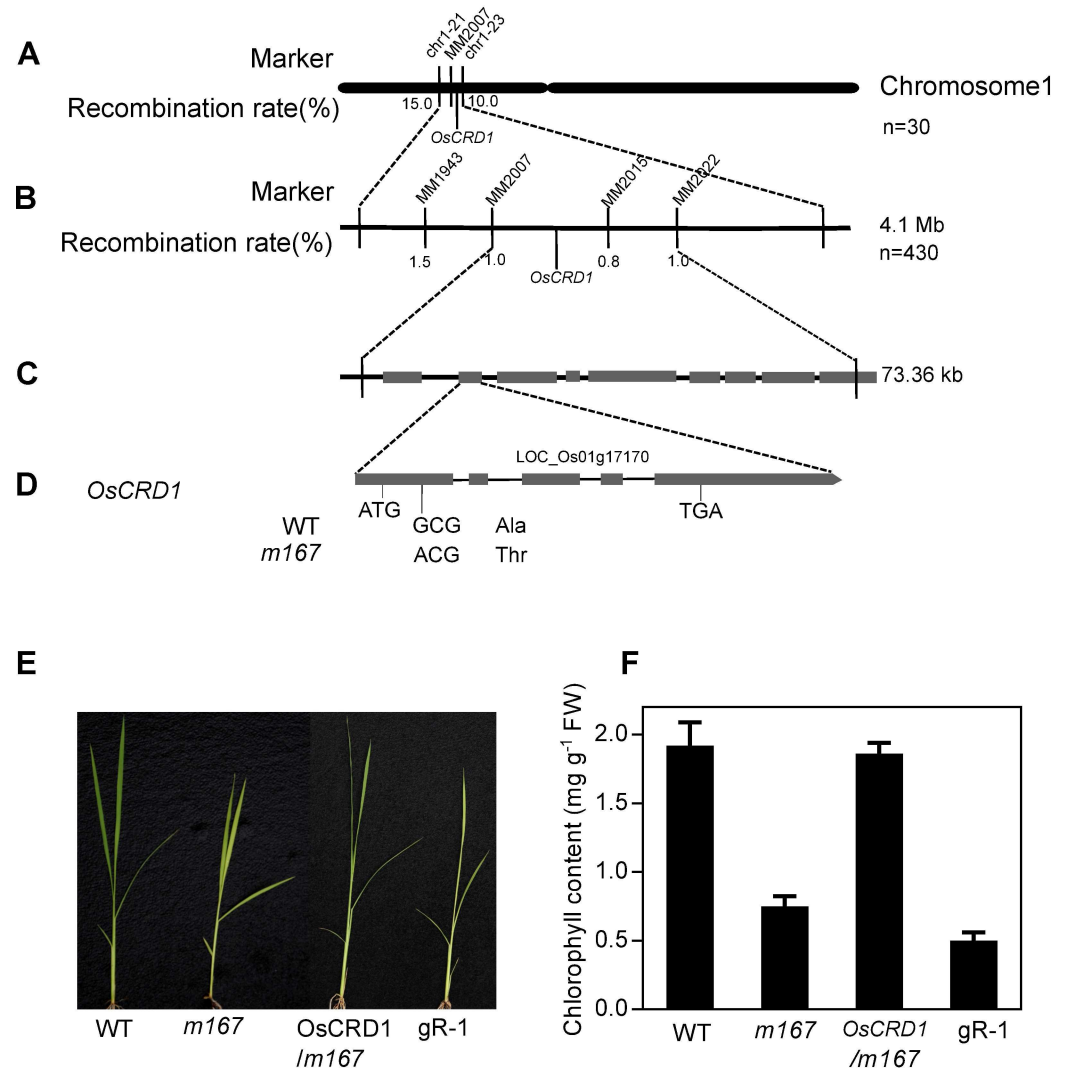


Fig 4. Map-based cloning of *OsCRD1* in *m167*. A, The candidate gene was mapped to a region between SSR markers Chr1-21 and Chr1-23 on chromosome 1. B, The target region was narrowed to a 73.36-kb region between SSR markers MM2007 and MM2022. C, There are nine ORFs between MM2007 and MM2022, including LOC_Os01g17160, LOC_Os01g17170, LOC_Os01g17180, LOC_Os01g17190, LOC_Os01g17214, LOC_Os01g17240, LOC_Os01g17250, LOC_Os01g17260, LOC_Os01g17279, respectively (from left to right). D, Structure of *OsCRD1* gene. ATG and TGA represent the start and stop codons, respectively. Black boxes indicate the exons. A single G to A substitution in the first exon in *m167*. E, Seedlings of *m167* complemented with wild type *OsCRD1* genomic sequence (*OsCRD1/m167*) and edited in *OsCRD1* coding sequence of wild type by CRISPR-Cas9 method (2gR-1). F, Chlorophyll concentration of seedlings shown in E. Pictures are representative photos of 3 independent transgenic lines with similar results. Values are means \pm SD with 3 independent transgenic lines.

doi:10.1371/journal.pone.0171118.g004

reading frame (ORF) of 1227 bp encoding a 408-amino acid protein with molecular mass 47.3 KDa.

Multiple amino acid sequence alignment indicated that *OsCRD1* has higher sequence similarity in all species. The MPEC subunit encoded by *OsCRD1* has more than 80% identity with other orthologs in green algae, bryophyte and higher green plants (S2 Fig), including CHL27 in *Arabidopsis*, suggesting that it is a highly conserved protein and might be essential for photosynthesis. Sequence alignment indicated that the mutation of *OsCRD1* in *m167* is highly conserved in different green plants and rice varieties (S2 and S3 Figs).

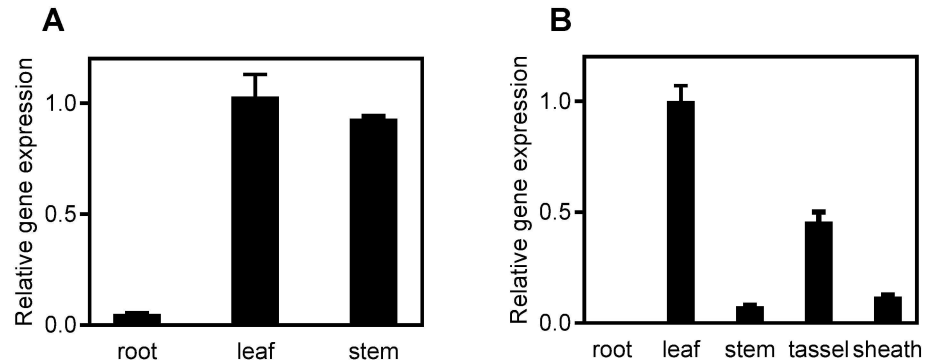


Fig 5. Expression analysis of *OsCRD1*. A. *OsCRD1* gene expression at seedling stage. B. *OsCRD1* gene expression at heading stage. Expression of *OsCRD1* in leaves was analyzed using quantitative RT-PCR. Osactin gene was used as an internal control. Data are means \pm SD (n = 3).

doi:10.1371/journal.pone.0171118.g005

OsCRD1 is mainly expressed in green tissues

Quantitative real-time PCR analysis showed that *OsCRD1* is mainly expressed in green tissues including stem, leaf, tassel and sheath but not in root (Fig 5). The expression in leaf was relatively high, while the expression in root was almost undetectable or at a very low level. A single nucleotide G-to-A substitution in *OsCRD1* leads to its expression downregulation in *m167* compared with WT plants (S4 Fig).

OsCRD1 protein localizes in chloroplast

To determine the subcellular location of *OsCRD1* protein, we constructed *OsCRD1-GFP* vector for transient expression in rice protoplasts mediated by PEG. Confocal microscopy analysis of *OsCRD1-GFP* location showed that *OsCRD1* is localized in chloroplast (Fig 6). To test whether *OsCRD1* Ala 96 to Thr (*OsCRD1A96T*) mutation in *m167* affected the subcellular localization, we also performed a transient expression analysis of the *OsCRD1A96T-GFP* fusion protein. *OsCRD1A96T* mutant proteins were localized in chloroplast (S5 Fig), indicating the *OsCRD1A96T* mutation does not affect protein localization.

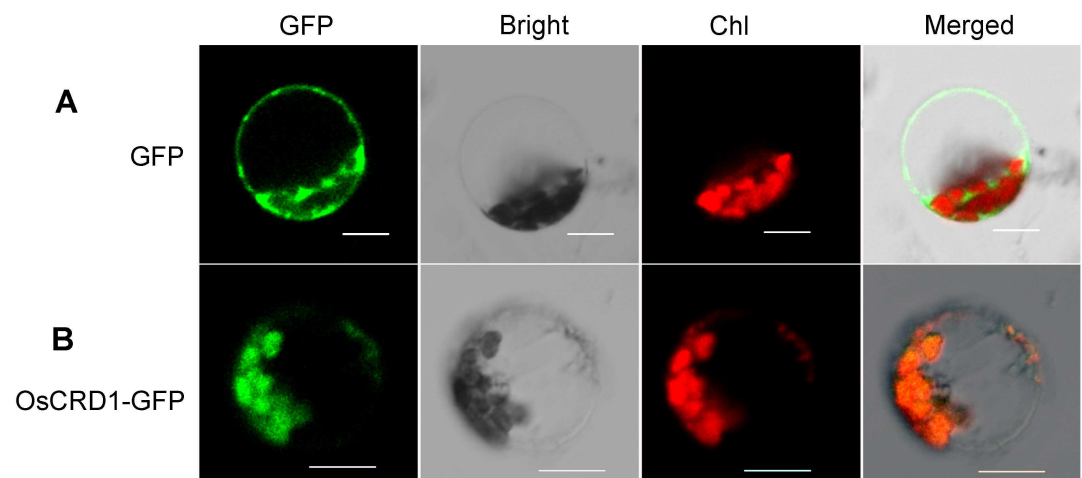


Fig 6. Subcellular localization of *OsCRD1* in rice protoplast. A, Fluorescence localization of free GFP in rice protoplast. B, Fluorescence localization of *OsCRD1-GFP* fused protein in rice protoplast.

doi:10.1371/journal.pone.0171118.g006

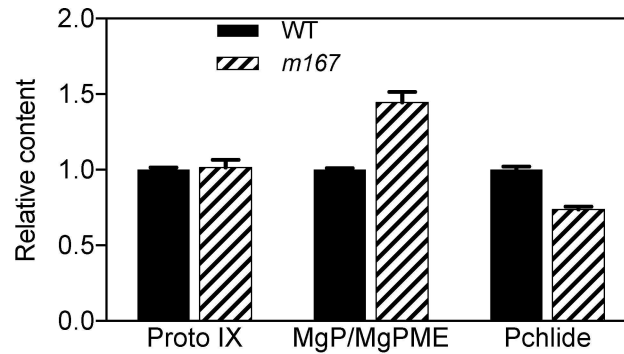


Fig 7. Analysis of chlorophyll (Chl) intermediates Proto IX, MgP/MgPME and Pchlde in WT and *m167* mutant.

doi:10.1371/journal.pone.0171118.g007

Mutation in OsCRD1 impaired MPEC activity

The yellow-green leaf phenotype of *m167* suggested that Chl biosynthesis in *m167* mutant might be damaged. So we determined the intermediates Proto IX, MgP/MgPME and Pchlde in Chl biosynthesis (Fig 7). Compared to WT, Proto IX was slightly increased in *m167* mutant, and MgP/MgPME were increased by 44% in *m167* mutant. However, Pchlde was decreased by about 30% in *m167* mutant (Fig 7). Therefore, the increase of MgP/MgPME and decrease of Pchlde in *m167* mutant indicate that the cyclase activity of MPEC was damaged in *m167* mutant possibly by a mutation in OsCRD1.

Discussion

Chlorophylls are essential for photosynthesis and plant growth. Chlorophyll biosynthesis is a highly coordinated process that is executed via a series of cooperative reactions catalyzed by numerous enzymes. However, only several genes have been studied in rice. In this study, we characterized a yellow-green leaf rice mutant *m167*. By map-based cloning, we cloned the mutation gene *OsCRD1*, encoding a putative subunit of MPEC, the most enigmatic enzyme in chlorophyll biosynthesis.

Similar to previous identified abnormal leaf color mutants [33–38], chloroplast development in *m167* is impaired, which indicates that the chlorophyll synthesis is co-regulated with chloroplast development [39]. Chlorophyll molecules absorb light in photosystems embedded in the chloroplast thylakoid membranes, therefore, lack of chlorophyll might impair the photosynthetic performance. Whether there is any specific regulatory function of CRD1 or MPEC enzyme on photosynthetic functions is an interesting topic to be addressed in the future.

In *Arabidopsis*, leaves of *gun4* mutant range from albino to pale green to yellow-green under normal growth conditions [40–42]. In *Arabidopsis* GUN4 promotes the activity of Mg-chelatase, upstream of MPEC in chlorophyll biosynthesis pathway [42, 43]. Whether OsGUN4 regulates MPEC in rice is to be investigated in future studies.

Previous studies revealed that MPEC is a multimeric enzyme in green algae and plants, and its activity requires several components. In our study, we found that yellow-green plants of *m167* did not accumulate Pchlde when fed 5-ALA in the dark as WT plants, indicating OsCRD1 might participate in Chl biosynthesis. In *m167* mutant, MgPME accumulated and Pchlde decreased, which implied that *m167* is deficient in the cyclase [11, 15]. We incubated the purified recombinant OsCRD1 from *E. coli* with the substrate MProtoME in the reaction buffer, but did not detect the production of Pchlde after incubation, possibly resulting from

the lack of other components of MPEC [9–11]. Thus, the biochemical property of MPEC needs to be confirmed, and its regulation mechanism is still unknown in rice yet.

Supporting Information

S1 Fig. Sequencing confirmation for complementation of *m167* with WT *OsCRD1* genomic sequence (A) and knocking out of *OsCRD1* in wild type Kitaake (B).
(PDF)

S2 Fig. Sequence alignment of *OsCRD1* protein and its related proteins.
(PDF)

S3 Fig. Sequence analysis of *OsCRD1* in different rice varieties.
(PDF)

S4 Fig. Expression of *OsCRD1* gene in 2-week seedlings of WT and *m167*.
(PDF)

S5 Fig. Subcellular localization of *OsCRD1A96T* in rice protoplasts.
(PDF)

S1 Table. Sequences of the primers used in this study.
(DOC)

S2 Table. Nine candidate genes annotated in mapping region.
(DOC)

Acknowledgments

This work was supported by Ministry of Agriculture of China (2014ZX08009-005, 2016ZX08009-003-005) and National Natural Science Foundation of China (31172025).

Author Contributions

Conceptualization: RQ RH.

Formal analysis: XW RQ RH.

Funding acquisition: RQ RH.

Investigation: XW.

Project administration: RQ RH.

Resources: RQ RH.

Supervision: RQ RH.

Writing – original draft: XW RQ.

Writing – review & editing: XW RQ.

References

1. Caffarri S, Tibiletti T, Jennings RC, Santabarbara S. A comparison between plant photosystem I and photosystem II architecture and functioning. *Curr. Protein Pept. Sci.* 2014; 15(4):296–331. doi: [10.2174/1389203715666140327102218](https://doi.org/10.2174/1389203715666140327102218) PMID: [24678674](https://pubmed.ncbi.nlm.nih.gov/24678674/)
2. Von Wettstein D, Gough S, Kannangara CG. Chlorophyll biosynthesis. *Plant Cell* 1995; 7:1039–1057. doi: [10.1105/tpc.7.7.1039](https://doi.org/10.1105/tpc.7.7.1039) PMID: [12242396](https://pubmed.ncbi.nlm.nih.gov/12242396/)

3. Bollivar DW. Recent advances in chlorophyll biosynthesis. *Photosynth. Res.* 2006; 90(2):173–94. PMID: [17370354](#)
4. Tanaka R, Tanaka A. Tetrapyrrole biosynthesis in higher plants. *Annu. Rev. Plant Biol.* 2007; 58(1):321–346.
5. Tanaka R, Kobayashi K, Masuda T. Tetrapyrrole metabolism in *Arabidopsis thaliana*. *The Arabidopsis Book* 2011:e0145–. doi: [10.1199/tab.0145](#) PMID: [22303270](#)
6. Schlicke H, Richter A, Rothbart M, Brzezowski P, Hedtke B, Grimm B. Function of tetrapyrroles, regulation of tetrapyrrole metabolism and methods for analyses of tetrapyrroles. *Procedia Chem.* 2015; 14:171–175.
7. Brzezowski P, Richter AS, Grimm B. Regulation and function of tetrapyrrole biosynthesis in plants and algae. *Biochim. Biophys. Acta* 2015; 1847:968–985. doi: [10.1016/j.bbabi.2015.05.007](#) PMID: [25979235](#)
8. Walker C, Mansfield K, Smith K, Castelfranco P. Incorporation of atmospheric oxygen into the carbonyl functionality of the protochlorophyllide isocyclic ring. *Biochem. J.* 1989; 257(2):599–602. PMID: [2930469](#)
9. Wong YS, Castelfranco PA. Resolution and reconstitution of Mg-protoporphyrin IX monomethyl ester (oxidative) cyclase, the enzyme system responsible for the formation of the chlorophyll isocyclic ring. *Plant Physiol.* 1984; 75:658–661. PMID: [16663682](#)
10. Walker CJ, Castelfranco PA, Whyte BJ. Synthesis of divinyl protochlorophyllide. Enzymological properties of the Mg-protoporphyrin IX monomethyl ester oxidative cyclase system. *Biochem. J.* 1991; 276:691–697. PMID: [1905926](#)
11. Pinta V, Picaud M, Reiss-Husson F, Astier C. *Rubrivivax gelatinosus acsF* (previously *orf358*) codes for a conserved, putative binuclear-iron-cluster-containing protein involved in aerobic oxidative cyclization of Mg-protoporphyrin IX monomethylester. *J. Bacteriol.* 2002; 184:746–753. doi: [10.1128/JB.184.3.746-753.2002](#) PMID: [11790744](#)
12. Moseley J, Quinn J, Eriksson M, Merchant S. The *Crd1* gene encodes a putative di-iron enzyme required for photosystem I accumulation in copper deficiency and hypoxia in *Chlamydomonas reinhardtii*. *EMBO J.* 2000; 19(10):2139–2151. doi: [10.1093/emboj/19.10.2139](#) PMID: [10811605](#)
13. Zheng C, Porat R, Lu P, O'Neill S. *PNZIP* is a novel mesophyll-specific cDNA that is regulated by phytochrome and the circadian rhythm and encodes a protein with a leucine zipper motif. *Plant Physiol.* 1998; 116(1):27–35. PMID: [9449833](#)
14. Hung CY, Sun YH, Chen J, Darlington DE, Williams AL, Burkey KO, et al. Identification of a Mg-protoporphyrin IX monomethyl ester cyclase homologue, EaZIP, differentially expressed in variegated *Epipremnum aureum* 'Golden Pothos' is achieved through a unique method of comparative study using tissue regenerated plants. *J. Exp. Bot.* 2010; 61(5):1483–1493. doi: [10.1093/jxb/erq020](#) PMID: [20167611](#)
15. Tottey S, Block MA, Allen M, Westergren T, Albrieux C, Scheller HV, et al. *Arabidopsis* CHL27, located in both envelope and thylakoid membranes, is required for the synthesis of protochlorophyllide. *Proc. Natl. Acad. Sci. U.S.A.* 2003; 100(26):16119–16124. doi: [10.1073/pnas.2136793100](#) PMID: [14673103](#)
16. Rzeznicka K, Walker CJ, Westergren T, Kannangara CG, von Wettstein D, Merchant S, et al. *Xantha-I* encodes a membrane subunit of the aerobic Mg-protoporphyrin IX monomethyl ester cyclase involved in chlorophyll biosynthesis. *Proc. Natl. Acad. Sci. U.S.A.* 2005; 102(16):5886–5891. doi: [10.1073/pnas.0501784102](#) PMID: [15824317](#)
17. Bang WY, Jeong IS, Kim DW, Im CH, Ji C, Hwang SM, et al. Role of *Arabidopsis* CHL27 protein for photosynthesis, chloroplast development and gene expression profiling. *Plant Cell Physiol.* 2008; 49(9):1350–1363. doi: [10.1093/pcp/pcn111](#) PMID: [18682427](#)
18. Albus CA, Salinas A, Czarnecki O, Kahlau S, Rothbart M, Thiele W, et al. LCAA, a novel factor required for magnesium protoporphyrin monomethylester cyclase accumulation and feedback control of aminolevulinic acid biosynthesis in tobacco. *Plant Physiol.* 2012; 160(4):1923–1939. doi: [10.1104/pp.112.206045](#) PMID: [23085838](#)
19. Hollingshead S, Kopečná J, Jackson PJ, Canniffe DP, Davison PA, Dickman MJ, et al. Conserved chloroplast open-reading frame ycf54 is required for activity of the magnesium protoporphyrin monomethylester oxidative cyclase in *Synechocystis* PCC 6803. *J. Biol. Chem.* 2012; 287(33):27823–27833. doi: [10.1074/jbc.M112.352526](#) PMID: [22711541](#)
20. Bollivar D, Braumann I, Berendt K, Gough SP, Hansson M. The Ycf54 protein is part of the membrane component of Mg-protoporphyrin IX monomethyl ester cyclase from barley (*Hordeum vulgare* L.). *FEBS J.* 2014; 281(10):2377–2386. doi: [10.1111/febs.12790](#) PMID: [24661504](#)
21. Johnson M, Zaretskaya I, Raytselis Y, Merezuk Y, McGinnis S, Madden TL. NCBI BLAST: a better web interface. *Nucleic Acids Res.* 2008; 36(Web Server issue):W5–W9. doi: [10.1093/nar/gkn201](#) PMID: [18440982](#)

22. Porra RJ. The chequered history of the development and use of simultaneous equations for the accurate determination of chlorophylls a and b. *Photosynth. Res.* 2002; 73(1–3):149–156. doi: [10.1023/A:1020470224740](https://doi.org/10.1023/A:1020470224740) PMID: [16245116](https://pubmed.ncbi.nlm.nih.gov/16245116/)
23. Schreiber U, Bilger W, Neubauer C. Chlorophyll fluorescence as a noninvasive indicator for rapid assessment of in vivo photosynthesis. In: *Ecophysiology of Photosynthesis*. ed. by Schulze ED, Caldwell MM Berlin, Heidelberg: Springer Berlin Heidelberg, 1995:49–70.
24. Park SY, Yu JW, Park JS, Li J, Yoo SC, Lee NY, et al. The senescence-induced staygreen protein regulates chlorophyll degradation. *Plant Cell* 2007; 19:1649–1664. doi: [10.1105/tpc.106.044891](https://doi.org/10.1105/tpc.106.044891) PMID: [17513504](https://pubmed.ncbi.nlm.nih.gov/17513504/)
25. Zhang Y, Su J, Duan S, Ao Y, Dai J, Liu J, et al. A highly efficient rice green tissue protoplast system for transient gene expression and studying light/chloroplast-related processes. *Plant Methods* 2011; 7(1):30. doi: [10.1186/1746-4811-7-30](https://doi.org/10.1186/1746-4811-7-30) PMID: [21961694](https://pubmed.ncbi.nlm.nih.gov/21961694/)
26. Hodgins RR, Huystee RBV. Rapid simultaneous estimation of protoporphyrin and Mg-Porphyrins in higher plants. *Plant Physiol.* 1986; 125(3–4): 311–323.
27. Gough S. Defective synthesis of porphyrins in barley plastids caused by mutations in nuclear genes. *Biochim Biophys Acta.* 1972; 286(1): 36–54. PMID: [4659262](https://pubmed.ncbi.nlm.nih.gov/4659262/)
28. Kahn VM, Avivi-Bieise, von Wettstein D. Genetic regulation of chlorophyll synthesis analyzed with mutants in barley. In Buchler J, ed, *Genetics and Biogenesis of Chloroplasts and Mitochondria*. 1976; 184(4138): pp800–802.
29. Mascia P. An analysis of precursors accumulated by several chlorophyll biosynthetic mutants of maize. *Molec. Gen. Genet.* 1978; 161(3): 237–244.
30. Duggan J, Gassman M. Induction of porphyrin synthesis in etiolated bean leaves by chelators of iron. *Plant Physiol.* 1974; 53(2): 206–215. PMID: [16658677](https://pubmed.ncbi.nlm.nih.gov/16658677/)
31. Xing HL, Dong L, Wang ZP, Zhang HY, Han CY, Liu B, et al. A CRISPR/Cas9 toolkit for multiplex genome editing in plants. *BMC Plant Biol.* 2014; 14:327. doi: [10.1186/s12870-014-0327-y](https://doi.org/10.1186/s12870-014-0327-y) PMID: [25432517](https://pubmed.ncbi.nlm.nih.gov/25432517/)
32. Shan Q, Wang Y, Li J, Gao C. Genome editing in rice and wheat using the CRISPR/Cas system. *Nat. Protoc.* 2014; 9(10):2395–2410. doi: [10.1038/nprot.2014.157](https://doi.org/10.1038/nprot.2014.157) PMID: [25232936](https://pubmed.ncbi.nlm.nih.gov/25232936/)
33. Zhang H, Li J, Yoo JH, Yoo SC, Cho SH, Koh HJ, et al. Rice *Chlorina-1* and *Chlorina-9* encode ChlD and ChlI subunits of Mg-chelatase, a key enzyme for chlorophyll synthesis and chloroplast development. *Plant Mol. Biol.* 2006; 62(3):325–337. doi: [10.1007/s11103-006-9024-z](https://doi.org/10.1007/s11103-006-9024-z) PMID: [16915519](https://pubmed.ncbi.nlm.nih.gov/16915519/)
34. Sakuraba Y, Rahman ML, Cho SH, Kim YS, Koh HJ, Yoo SC, et al. The rice *faded green leaf* locus encodes protochlorophyllide oxidoreductase B and is essential for chlorophyll synthesis under high light conditions. *Plant J.* 2013; 74:122–133. doi: [10.1111/tpj.12110](https://doi.org/10.1111/tpj.12110) PMID: [23289852](https://pubmed.ncbi.nlm.nih.gov/23289852/)
35. Zhou K, Ren Y, Lv J, Wang Y, Liu F, Zhou F, et al. *Young Leaf Chlorosis 1*, a chloroplast-localized gene required for chlorophyll and lutein accumulation during early leaf development in rice. *Planta* 2013; 237(1):279–292. doi: [10.1007/s00425-012-1756-1](https://doi.org/10.1007/s00425-012-1756-1) PMID: [23053539](https://pubmed.ncbi.nlm.nih.gov/23053539/)
36. Li RQ, Huang JZ, Zhao HJ, Fu HW, Li YF, Liu GZ, et al. A down-regulated epiallele of the *genomes uncoupled 4* gene generates a *xantha* marker trait in rice. *Theor. Appl. Genet.* 2014; 127(11):2491–2501. doi: [10.1007/s00122-014-2393-9](https://doi.org/10.1007/s00122-014-2393-9) PMID: [25208645](https://pubmed.ncbi.nlm.nih.gov/25208645/)
37. Wu Z, Zhang X, He B, Diao L, Sheng S, Wang J, et al. A chlorophyll-deficient rice mutant with impaired chlorophyllide esterification in chlorophyll biosynthesis. *Plant Physiol.* 2007; 145(1):29–40. doi: [10.1104/pp.107.100321](https://doi.org/10.1104/pp.107.100321) PMID: [17535821](https://pubmed.ncbi.nlm.nih.gov/17535821/)
38. Zhu X, Guo S, Wang Z, Du Q, Xing Y, Zhang T, et al. Map-based cloning and functional analysis of *YGL8*, which controls leaf colour in rice (*Oryza sativa*). *BMC Plant Biol.* 2016; 16:134. doi: [10.1186/s12870-016-0821-5](https://doi.org/10.1186/s12870-016-0821-5) PMID: [27297403](https://pubmed.ncbi.nlm.nih.gov/27297403/)
39. Biswal UC, Biswal B, Raval MK. Protoplastid to chloroplast transformation. In: *Chloroplast biogenesis. From proplastid to gerontoplast*. Kluwer Academic Publishers, 2003:19–77.
40. Larkin RM, Alonso JM, Ecker JR, Chory J. GUN4, a regulator of chlorophyll synthesis and intracellular signaling. *Science* 2003; 299:902–906. doi: [10.1126/science.1079978](https://doi.org/10.1126/science.1079978) PMID: [12574634](https://pubmed.ncbi.nlm.nih.gov/12574634/)
41. Peter E, Grimm B. GUN4 is required for posttranslational control of plant tetrapyrrole biosynthesis. *Mol. Plant* 2009; 2:1198–1210. doi: [10.1093/mp/ssp072](https://doi.org/10.1093/mp/ssp072) PMID: [19995725](https://pubmed.ncbi.nlm.nih.gov/19995725/)
42. Adhikari ND, Froehlich JE, Strand DD, Buck SM, Kramer DM, Larkin RM. GUN4-porphyrin complexes bind the ChlH/GUN5 subunit of Mg-Chelatase and promote chlorophyll biosynthesis in *Arabidopsis*. *Plant Cell* 2011; 23:1449–1467. doi: [10.1105/tpc.110.082503](https://doi.org/10.1105/tpc.110.082503) PMID: [21467578](https://pubmed.ncbi.nlm.nih.gov/21467578/)
43. Porra RJ. Recent progress in porphyrin and chlorophyll biosynthesis. *Photochem. Photobiol.* 1997; 65(3):492–516.